



## Better understanding of tide's influence on half-cell potential and electrical resistivity measurements for reinforced concrete in marine environment

Lucas Bourreau, Laurent Gaillet, Véronique Bouteiller, Franck Schoefs, Benoit Thauvin, Julien Schneider

### ► To cite this version:

Lucas Bourreau, Laurent Gaillet, Véronique Bouteiller, Franck Schoefs, Benoit Thauvin, et al.. Better understanding of tide's influence on half-cell potential and electrical resistivity measurements for reinforced concrete in marine environment. 40th IABSE Symposium: Tomorrow's Megastructures, Sep 2018, NANTES, France. 6 p. hal-02065141

**HAL Id: hal-02065141**

**<https://hal.science/hal-02065141v1>**

Submitted on 12 Mar 2019

**HAL** is a multi-disciplinary open access archive for the deposit and dissemination of scientific research documents, whether they are published or not. The documents may come from teaching and research institutions in France or abroad, or from public or private research centers.

L'archive ouverte pluridisciplinaire **HAL**, est destinée au dépôt et à la diffusion de documents scientifiques de niveau recherche, publiés ou non, émanant des établissements d'enseignement et de recherche français ou étrangers, des laboratoires publics ou privés.



## Better understanding of tide's influence on half-cell potential and electrical resistivity measurements for reinforced concrete in marine environment

**Lucas Bourreau**

*SIXENSE Concrete, Agence Ouest, F44115 Haute-Goulaine, France*

**Laurent Gaillet**

*Université Bretagne Loire, IFSTTAR, MAST, SMC, F44344 Bouguenais, France*

**Véronique Bouteiller**

*Université Paris-Est, MAST, EMGCU, IFSTTAR, 77447 Marne-la-Vallée, France*

**Franck Schoefs**

*Université Bretagne Loire, Université de Nantes, GeM, UMR CNRS 6183, Research Institute in Civil Engineering and Mechanics, France, IUML FR CNRS 3473, Sea and Littoral research Institute, Nantes, France*

**Benoit Thauvin**

*Cerema Ouest, F22015 Saint-Brieuc, France*

**Julien Schneider**

*Cerema Ile-de-France, F77171 Sourdun, France*

Contact: [laurent.gaillet@ifsttar.fr](mailto:laurent.gaillet@ifsttar.fr)

### Abstract

Main damage occurring on reinforced concrete (RC) structures can be attributed to the corrosion of the rebar. Chloride ions penetration and/or carbonation, as major causes of RC corrosion, are well understood for onshore structures. When dealing with structures in marine environment, more parameters must be considered, as the different exposure zones (tidal, splash and atmospheric) will have a significant influence on the corrosion behavior.

This article deals with the corrosion diagnosis of the piers of the ile de Ré bridge. The objective is to provide an effective method to identify the different exposure zones based on the non-destructive measurements (half-cell potential) that are modelled taking into account the influence of the tide.

**Keywords:** reinforced concrete, bridge, marine environment, corrosion diagnosis, concrete durability, half-cell potential

## 1 Introduction

Corrosion is the main cause of degradation of reinforced concrete structures [1-3]. This later is relatively well known for atmospheric structures but many other parameters are involved in marine conditions, including the different exposure zones [4-6]. Non-destructive techniques for corrosion evaluation of rebars are more difficult to apply in this case in order to establish a corrosion diagnosis [7-9].

In this article are presented results from half-cell potential measurements obtained on the piers of the Ile de Ré Bridge. An innovative data processing method is used to identify the different exposure zone heights taking into account the influence of the tide on the results.

## 2 Material and methods

The corrosion measurements were performed on a set of piers of the ile de Ré bridge on the Atlantic coast. Two sides of the piers (Side C and side G) were considered corresponding to different environmental conditions. Assessment zone included 3 different exposure zones (tidal, splash and atmospheric) with 1m height each and 1.85 m width. A complete corrosion diagnosis methodology was established consisting in different stages [10]. Corrosion diagnosis was performed using a vessel. Half-cell potential measurements were performed using a Canin+® device (: copper/saturated copper sulphate electrode)

## 3 Results

### 3.1 Corrosion diagnosis

Performing a corrosion diagnosis is not obvious on reinforced structures in a marine environment and the interpretation of the results can be tricky. Fig 1 represents the half-cell potential mapping of the investigated area analysed with the ASTM C876-91 standard [11, all the values done on the pier's zones with heights lower than a given value would refer to a high probability of corrosion (Fig. 1) as

potential values are less than -350 mV/CSE and therefore can be attributed to a probability of corrosion superior to 90% (Fig. 1). For the same experimental data, the interpretation based on COST-509 or RILEM TC 154 documents also lead to erroneous conclusions that were not supported by the visual inspection observations [7] [12].

This half-cell potential map (fig 1) can be explained by the fact that high negative values correspond to rebar situated in the tidal zone where the concrete is saturated of sea water and there is a lack of oxygen [11, 13-15]. Above the tidal zone, concrete is less saturated and more oxygenated and therefore potential values are in a medium range.

These very negative potentials can be attributed to an active corrosion but also to the marine environment for structures in submerged or in tidal zones. So, a method is proposed to withdraw the tide's effect on the measured potentials.

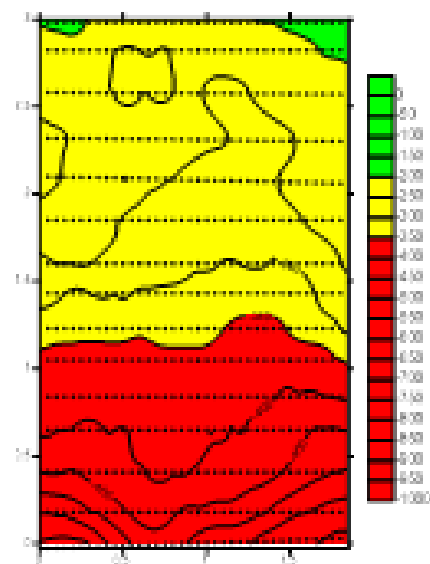


Figure 1: Half-cell potential map of a passive pier's side, using the ASTM recommendation.

### 3.2 Enhanced corrosion diagnosis

To study and quantify the tide's effect on the potential measurements, mean trends of a dataset of potential values have been computed. This

selected dataset corresponds to pier sides where no corrosion has been detected.

### 3.3 Tide's effect on potential values

The mean value ( $\mu_{Ecorr}$ ) and the standard deviation ( $\sigma_{Ecorr}$ ) have been calculated for each horizontal measurement lines. In order to delete the outlier values from the main trend, the absolute values which were not included in the range defined by  $\mu \pm 3\sigma$  were deleted of the dataset. Figure 2 presents the mean potential trend for the selected pier sides versus water height.

Different evolution's behaviour (dashed coloured lines) can be observed on Figure 2 that can be related to the exposure zones.

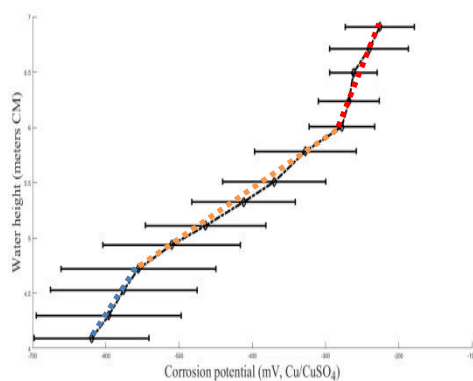


Figure 2: Mean potential trend versus water height (based on four selected pier sides of the bridge).

A first statement is that a change of behaviour in the mean trend represents the transition from an exposure zone to another, which corresponds to a boundary between two exposure zones. A data classification method was used to identify the transitions based on an analysis that focused on the slope's values computed from two adjacent potential mean values. The dataset consisted in the two sides of the piers as exposure zones locations are assumed not to be dependent on surface concrete conditions.

After dataset has been normalized, K-means classification algorithm has been applied to determine a modification of the value's evolution into mean trends. The optimal number of cluster was determined using the Caliński-Harabasz

criterion [16]. The number of cluster ( $k$ ) is optimal when the Caliński-Harabasz criterion is maximal. This analysis has been reiterated for all seasons. An overall optimal number of clusters of 3 is determined and will be considered in the following.

Boundaries between two exposure zones are located between two slopes values. Using the classification results, an identification and location of these boundaries is achievable. Boundaries between the high and median zones are located at water height 6.12 – 5.64 m CD and 5.02 – 4.62 m CD for potential values.

These calculated values for exposure zones and their boundaries have been compared to "physical" values for steel structures in marine conditions according to literature (Tab. 1) [29].

Table 1: Comparison between positions of exposures zones defined for steel structures and

Metallic structures		
zones	Water height (+ m CD)	Tidal coefficient
Atmospheric and splash zones	6.00	95
Splash and tidal zones	5.45	70
Reinforced concrete structures piers		
Boundaries between zones	Water height (+ m CD)	Tidal coefficient
High and median	6.12 – 6.00	101 – 95
Median and low	5.02 – 4.92	51 – 46

those calculated for RC piers.

Boundaries between atmospheric and splash zones for steel structures, between high and median zones for RC structures are alike. A more important difference exists between splash-tidal zones

boundary for steel structures and median-low zones boundary for RC structures. This boundary difference may be put in relation with 2 explanations: boundaries for steel structures are theoretic values and corrosion behavior is quite different for RC structures.

As a result of this comparison; the low, median and high zones are attributed to the tidal, splash and atmospheric exposure zones respectively.

### 3.4 Tide's effect quantification

As an assumption, concrete's exposition to the wetting/drying cycles is considered as the origin for tide's effect on half-cell potential data. From this point of view, the two sides of the pier have different behaviours and must be studied separately. A side C (most exposed to wetting/drying cycles) and G (less exposed to wetting/drying cycles) were labelled.

The same methodology as previously described was used to determine the mean trend of the potential values. Results are presented in Fig. 3 where the boundaries between the exposure zones are also indicated.

The modelling method was based on a fitting of every exposure zones by a linear regression in order to determine potential's evolution profiles as illustrated in Fig. 4

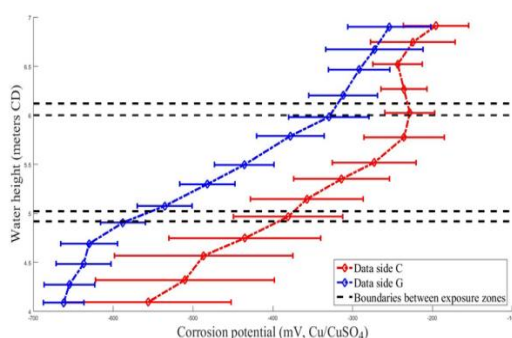


Figure 3: Mean potential trend versus water height for the 2 different sides of the piers of the bridge

Parameters of the linear regression have been determined and fits are significant with quite good  $R^2$  coefficients (0.66-1) for the potential data.

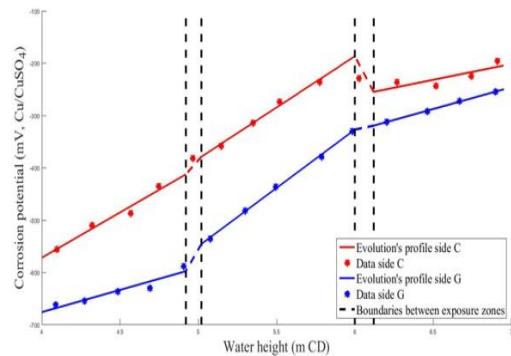


Figure 4: Evolution of potential profiles versus water height

From Figure 4, The potential values are more negative for side G than side C and this can be explained because side C is more exposed to wetting/drying cycles

This methodology of correction of initial potential data to withdraw the tide's effect on the corrosion potential has been tested on potential dataset previously analysed in paragraph 2 (Fig. 2). Reference corrosion potential calculated from the developed methodology are subtracted for every experimental potential value. The equicontour potential line plots from initial data and after using the developed methodology of correction are presented on Figure 5.

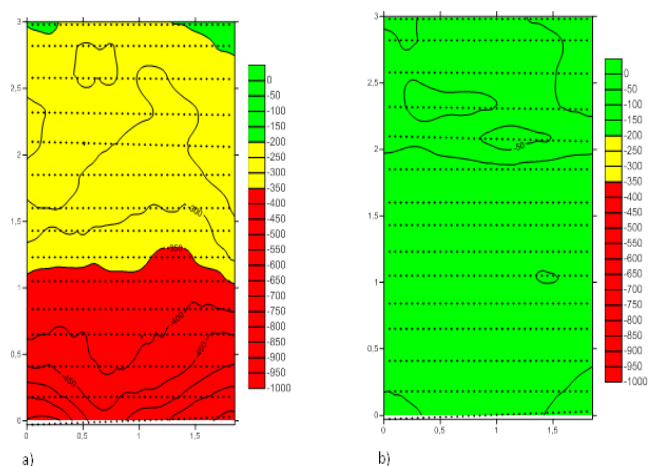


Figure 5: Half-cell potential maps of a passive pier's side, equicontour potential line plot using ASTM's recommendation with initial data (a) and corrected data (b).

Interpretation using the ASTM C876-91 standard is now different. In the earlier stage, a high probability of corrosion for lower heights and an

undefined risk of corrosion for the others zones were identified. After correction, the whole investigated area is associated to a low probability of corrosion.

## 4 Conclusions

Corrosion diagnosis of a reinforced concrete structure in the sea can result difficult because of the marine environment. In order to achieve a more reliable diagnosis based on half-cell potential measurements, a model was developed. First of all, the boundaries between tidal, splash and atmospheric zones were characterized and compared to the ones of metallic structures. Then, the influence of the tide was analysed and it was found that the evolution of the potential profiles versus water heights depended on the sides C or G of the piers and therefore of the exposure (more or less windy and humid). Finally, the develop methodology was efficient in obtaining corrected potential profiles (by substracting the tide effect) that were consistent with the standards or recommendation.

## Acknowledgements

The authors would like to thank the team of the DéCoF-Ré Project: B. Godart, W. Traverst, P. Boujard, N. Coulaty-Chin, A. Orcesi, Y. El Rabbih, X. Derobert, M. Sissoko (IFSTTAR); R. Queguiner, S. Pasquiet, P. Boulaire, M. Rebours, C. Naudat (Cerema Ouest); F. Landrin and V. Queyrat (Cerema Ile de France), J-F. Barthélémy (Cerema Dtech ITM); M. Roche, O. Amiri (Nantes University); M. Brouxel, S. Naar (SIXENSE-Concrete), A. Audouin-Dubreuil, F. Lavoute, M. Barbier (Département de la Charente-Maritime); F. Gazet (Dekra). They also thank the marine team for their help with the vessel.

## References

[1] Broomfield JP. Corrosion of steel in concrete - Understanding, investigation and repair. London: E&FN SPN; 1997.

[2] R. Cigna, C. Andrade, U. Nürnberger, R. Polder, R. Weydert, Seitz E, et al. COST 521 - Corrosion of steel in reinforced concrete structures - Final Report: European Communities, Luxembourg, EUR 20599; 2003.

[3] Poupard O, L'Hostis V, Bouteiller V, Capra B, Catinaud S, Francois D, et al. Corrosion diagnosis of reinforced concrete beams after 40 years exposure in marine environment by non destructive tools. *Revue Européenne de Génie Civil*. 2007;11(1-2):35-54.

[4] Costa, A. and Appleton, J., Chloride penetration into concrete in marine environment – Part I: Main parameters affecting chloride penetration, *Mater Struct* 32 (1999), 252-259

[5] Costa, A. and Appleton, J., Chloride penetration into concrete in marine environment – Part II: Prediction of long term chloride penetration, *Mater Struct* 32 (1999), 354-359

[6] Montemor, M. F., Chloride-induced corrosion on reinforcing steel: from the fundamentals to the monitoring techniques, *Cem Concr Compos* 25 (2003), 491-502

[7] Polder RB. Test methods for on site measurement of resistivity of concrete -a RILEM TC-154 technical recommendation. *Construction and Building Materials*. 2001;15(2-3):125-31.

[8] Andrade C, Alonso C. RILEM TC 154-EMC:Electrochemical Techniques for Measuring Metallic Corrosion - Recommendations - Test methods for on-site corrosion rate measurement of steel reinforcement in concrete by means of the polarization resistance method. *Materials and Structures*. 2004;37:623-43.

[9] Breyse D, Yotte S, Salta M, Schoefs F, Ricardo J, Chaplain M. Accounting for variability and uncertainties in NDT condition assessment of corroded RC-structures. *European Journal of Environmental and Civil Engineering*. 2009;13(5):573-91.

[10] Bourreau L. Diagnostic de corrosion sur ouvrage - Fiabilité et aide à la décision: Thèse de l'Université de Nantes, France; 2017.

[11] ASTM C876-91, Standard test method for half-cell potentials of uncoated reinforcing steel in

concrete, American Society for Testing and Materials, USA (1999)

[12] Cox RN, Cigna R, Vennesland O, Valente T, (Eds). COST 509 - Corrosion and protection of metals in contact with concrete - Final Report: European Commission, Directorate General Science, Research and Development, Brussels, EUR 17608 EN; 1997

[13] ASTM C876-09, Standard test method for half-cell potentials of uncoated reinforcing steel in concrete, American Society for Testing and Materials, USA (2009)

[14] Gonzalez, J. A. et al, Considerations on reproducibility of potential and corrosion rate measurements in reinforced concrete, Corr Sci 46 (2004), 2467-2485

[15] Hussain, R.R., Underwater half-cell corrosion potential bench mark measurement of corroding steel in concrete influenced by a variety of material science and environmental engineering variables, Measurement 44 (2011), 274-280

[17] Caliński T. and Harabasz J., A dendrite method for cluster analysis, Communications in Statistics-theory and Methods 3 (1974), 1-27.